PROCEEDINGS OF THE 17TH INTERNATIONAL CONFERENCE ON

OMAE

1998

OFFSHORE MECHANICS AND ARCTIC ENGINEERING

BOOK OF ABSTRACTS

PROCEEDINGS OF THE

17th International Offshore & Arctic Engineering Conference

July 5–9, 1998 • Lisbon, Portugal

OMAE'98

BOOK OF ABSTRACTS

Organized by

The Offshore Mechanics and Arctic Engineering (OMAE) Division, ASME

Portuguese Institute of Naval Architecture & Marine Engineering, Portugal

Sponsored by

The American Society of Mechanical Engineers (ASME), USA

Office of Science and Technology (OST), Australia

Royal Flemish Engineers Association (KVIV), Belgium

Canadian Petroleum Association (CPA), Canada

The Canadian Society for Mechanical Engineering (CSME), Canada

The Petroleum Society of CIM, Canada

Chinese Society of Ocean Engineers (CSOE), China

Dansk Ingenierforening (DIF), Denmark

European Safety and Relibility Association ESRA

Conseil de Liaison des Assoc. de Recherche sur les Ouvrages en Mer , France

Deutsches Komitee fur Meeresforschung und Meerestechnik, Germany

Institution of Engineers of Ireland (IEI), Ireland

Associazione Italiana di Ingegneria Offshore e Marina (AIOM), Italy

The Society of Naval Architects of Japan (SNAJ), Japan

The Japan Society of Mechanical Engineers (JSME), Japan

Korean Institute of Metals (KIM), Korea

Norwegian Society of Chartered Engineers (NIF), Norway

Portuguese Association of Engineers (ODE), Portugal

Institute of Materials (IM), UK

Institution of Mechanical Engineers (I.Mech.E.), UK

TWI (formerly The Welding Institute), UK

American Concrete Institute (ACI), USA

American Society of Civil Engineers (ASCE), USA

Energy Rubber Group (ACS), USA

National Association of Corrosion Engineers (NACE), USA

Engineering Committee on Oceanic Resources (ECOR)

THE AMERICAN SOCIETY OF MECHANICAL ENGINEERS

345 East 47th Street • New York, NY 10017

17th International Conference on
Offshore Mechanics and Arctic Engineering

OMAE98-0420

ANALYSIS OF DOUBLE-SKINNED CYLINDRICAL STRUCTURES BY THE STIFFENED PANEL METHOD

Philippe RIGO
ANAST, University of Liege, Belgium

Hengfeng WANG
ANAST, University of Liege, Belgium

ABSTRACT

The Stiffened Panel Method (SPM) is used to analyze double-skinned cylindrical structures. Governing equations of stiffened panels (sector plates and cylindrical shells) are obtained by using the effective unitary force method, in which the main slab is analyzed by the plate and shell theory, and the stiffeners are replaced by the effective unitary forces. With this method, stiffened panels can be analyzed exactly. For uniformly stiffened panels, the governing differential equations are greatly simplified by spreading the effective unitary forces over the panel. These simplified equations and their solutions are presented in an unified form valid for stiffened and unstiffened sector plates or cylindrical shells. In this way, all the panels can be analyzed by the same model. A double-skinned cylindrical structure composed of stiffened cylindrical shells and sector plates is treated as an assembly of the panels interconnected by the circumferential joints (nodes). Using Single Fourier Series (SFS) expanded in the circumferential direction, the general solutions of each panel for each SFS term are developed, which depend on 8 unknowns (4 node displacements at each end in the generator direction). An equation system on the node displacements of the whole structure is formed with the equilibrium equations at each node. This system is similar with those of standard numerical methods, such as the Finite Element Method (FEM). But, the dimension is much smaller. One single stiffened panel simulated by FEM will need thousands of DOFs (degree of freedom), while this method needs only 8 node displacements. Moreover, it is an exact theoretical solution.

The unit load solutions for each SFS term are defined as the fundamental solutions of the structure. Simply supported boundary conditions in the circumferential direction can be automatically simulated by SFS expansion, while other boundary conditions in the generator direction can vary arbitrarily. The global analysis of the concerned structure is realized by the superposition of the fundamental solutions for each SFS term. Additional boundary loads may overcome the limitation to the simply supported conditions in the circumferential direction. A package of FORTRAN code named LBR4C has been compiled according to the development. Both linear and nonlinear analyses can be performed. Only linear analyses are presented in this paper.

1. INTRODUCTION

Structures composed of stiffened panels are widely used in the modern world, such as ships, aircraft, hydraulic gates, steel bridges and so on. One of the methods to analyze this kind of structures, named **Stiffened Plate Method (SPM)**, was developed by N. M. Dehousse 1961. The governing differential equations of cylindrical shells with stiffeners in both generator and circumferential directions were developed. By using the Single Fourier Series expansion (abbreviated as SFS hereinafter) either in the generator direction (coordinate x) or in the circumferential direction (coordinate φ), the two-dimensional partial differential equations are transferred into the ordinary ones, and exact solutions are thus obtained. A computer program was compiled by N. M. Dehousse and J.Deprez 1967, which ran on IBM 7040 for a single stiffened plate panel. This is a great limitation, as most of the structures can not be analyzed by only one stiffened panel.

Prismatic structures composed of stiffened cylindrical shells and rectangular plates have been studied by Ph.Rigo 1989 with this method (rectangular plates are simulated by cylindrical shells with a small central angle). To design a prismatic structure, these stiffened panels (shells and plates) are interconnected by the joints along generator direction, and the SFS are expanded in the generator direction (coordinate x).

The main advantage of the method developed by Ph.Rigo concerns the discretization. "Panel" is the basic element of this method. Exact solutions of each panel are obtained theoretically, which depend on 4 end forces at each end in circumferential direction (8 end forces for two ends). A structure composed of N panels will have only 8*N unknowns (degree of freedom). It is evidently much smaller than with FEM analysis. For example, for FEM analysis of a single orthogonally stiffened plate panel, the number of DOFs (degree of freedom) ranges from 1917 to 3289, Hatzidakis, 1994. From this point of view, this method (Stiffened-Panel-Method) for multi-panel structures may be also named Finite-Panel-Method. Speed, simplicity and accuracy over mesh modeling have been demonstrated by the computer program named LBR4 with a large number of applications (Ph. Rigo 1992). This success encourages the authors to make further study by using this harmonic method.

This paper deals with a double-skinned cylindrical gate

proposed for the downstream gate of a high rise ship lock, shown in Fig.1, Dehousse 1989. The gate can be treated as an assembly of stiffened sector plates and cylindrical shells interconnected with the joints in the circumferential direction, see Fig.2. For this gate, the top, middle and bottom diaphragms are simulated with six stiffened sector plates (P1, P4, P7, P10, P13 and P16). The upstream and downstream skins are simulated with ten stiffened cylindrical shells (P2, P5, P8, P11, P14 for upstream skin and P3, P6, P9, P12, P15 for downstream skin). All together, sixteen panels, see Fig.2, are involved with 12 nodes (joints). The vertical diaphragms at $\varphi = 0$ and $\varphi = \varphi_0$ imply a simply supported boundary condition to the 16 studied panels.

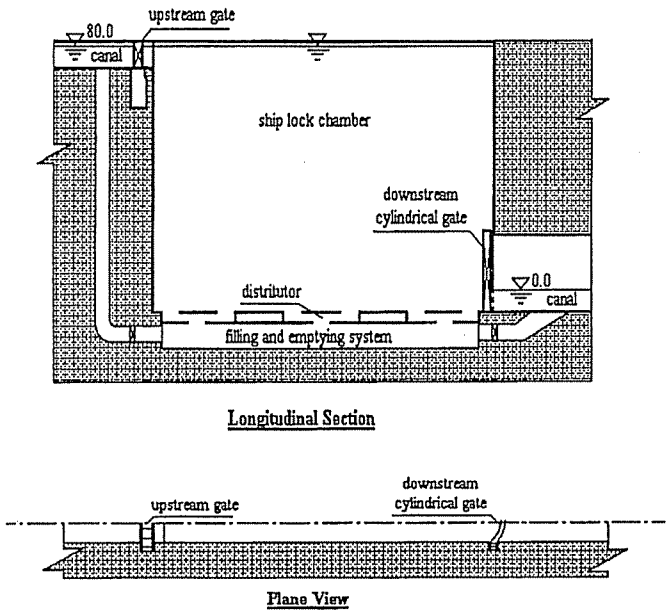

Fig.1 High Rise Ship Locks and Downstream Cylindrical Gate

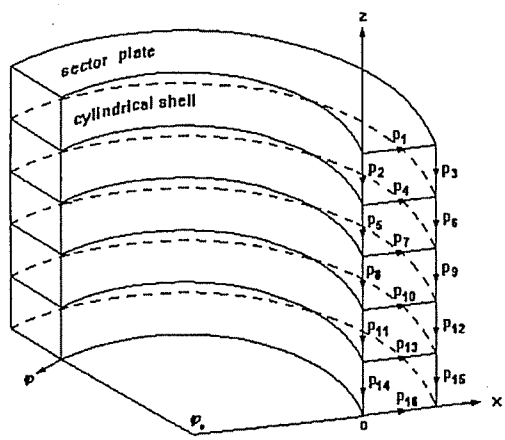

Fig.2 Model of Stiffened Panel Method

For this kind of the structures, all the panels can use the same coordinate φ in the circumferential direction (see Fig.2, the positive direction of the local coordinate x for each panel is shown by an arrow, and the local coordinate z is selected so that a right hand system, x-φ-z, is formed). Therefore, the SFS are expanded in the circumferential direction (coordinate φ) instead of the generator direction (coordinate x) for prismatic structures. The simply supported boundary conditions in the circumferential direction of the sector plates and the cylindrical shells are automatically satisfied by SFS expansion. Boundary conditions in the generator direction ($x = x_1$ and $x = x_2$) may arbitrarily vary from case to case.

Unstiffened sector plates had been a traditional mechanical research topic, especially for the lateral bending under external loads. However, for stiffened sector plates, the governing differential equations and their solutions have not yet been found in the available references. They have to be developed in this paper.

2. THEORY OF STIFFENED PANEL METHOD

The Stiffened Panel Method for curved structure is introduced in this paper, as such kind of structures can be treated as an assembly of stiffened sector plates and cylindrical shells. The SFS has to be expanded in the circumferential direction instead of the generator direction for prismatic structures. Theoretical solutions of each panel are first developed. Then, the structure is analyzed based on the connection among the panels.

2.1 SOLUTIONS OF STIFFENED PANELS

As one of the component of a structure or as a single panel structure, a thin-walled panel is usually reinforced with stiffeners because of strength or service requirements. In this research, as for most of real applications, only orthogonally distributed stiffeners are considered, which means that the stiffeners are arranged along the coordinate lines. The stiffeners in x direction are defined as stiffener x, and those in φ direction are defined as stiffener φ. As an example, one stiffened cylindrical shell (P3) and one stiffened sector plate (P4) of the studied structure are shown in Fig.3.

The governing differential equations of both stiffened sector plates and cylindrical shells can be obtained by using the effective unitary force method, Hengfeng Wang 1997. Based on the deformation of the main slab and the traditional beam theory, interaction forces at the joint of the main slab with the stiffeners are calculated on each stiffener. Adding these interaction forces into the governing equations of unstiffened panels, the governing differential equations of stiffened panels are formed. For uniformly stiffened panels (in which the stiffeners with identical sections in the same direction are uniformly arranged over the panel), these interaction forces can be spread over the panel if only the global rigidity of the panel is concerned. In this way, the governing differential equations of stiffened panels are greatly simplified. For both sector plates and cylindrical shells, they can be generalized as an unified form

$$\begin{bmatrix} a_1 & b_1 & c_1 \\ a_2 & b_2 & c_2 \\ a_3 & b_3 & c_3 \end{bmatrix} \cdot \begin{Bmatrix} U \\ V \\ W \end{Bmatrix} = \begin{Bmatrix} -X \\ -Y \\ Z \end{Bmatrix} \tag{1}$$

Here U, V and W are defined as the displacements of the middle surface of the main slab, and X, Y and Z stand for the external distributed loads. The positive directions of both the displacements and the external loads are the same as the local coordinates x-φ-z respectively, see Fig.3.

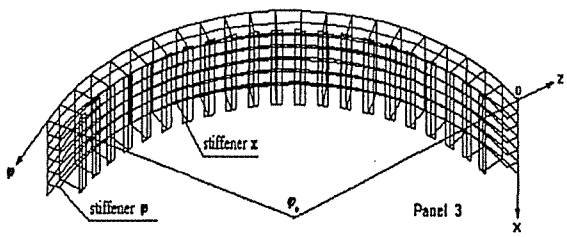

a. stiffened cylindrical shell

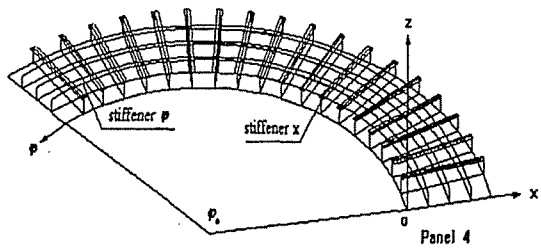

b. stiffened sector plate

Fig.3 Stiffened Panels and Their Coordinates

In Eq.(1), a1, a_2... are the corresponding differential operators, which vary with the shape of the studied panels and the coordinate system. Taking a_1 as an example, for **sector plate**, it has the form as

$$a_1U = (D+\bar{\omega}_x)U''+D\frac{U'}{x}-(D+\bar{\omega}_\varphi)\frac{U}{x^2}+\frac{\bar{S}_\varphi}{q^2}\frac{U^{\circ\circ\prime}}{x^3}+\left(\frac{1-\mu}{2}D-\frac{\bar{S}_\varphi}{q^2}\right)\frac{U^{\circ\circ}}{x^2}$$

For **cylindrical shells**, it takes the form as

$$a_1U = (D+\bar{\omega}_x)U''+\frac{1-\mu}{2}D\frac{U^{\circ\circ}}{q^2}$$

Hereinafter, we use $\frac{\partial(\ )}{\partial x}=(\ )'$ and $\frac{\partial(\ )}{\partial\varphi}=(\ )^\circ$. It should be also noted that all the operators for cylindrical shells are linear differential operators with constant coefficients, while those for sector plates are the non-linear ones, in which the term of 1/x and its power functions are included. This needs special treatment in mathematics.

Other operators and the formulas for strains, stresses and internal forces, which can be derived from the displacements, are not listed in this paper. But, what has to be mentioned is that the mechanical properties of the main slab and the stiffeners have been considered as accurate as possible in those equations. Moreover, simplifications have been made as less as possible. For instance, Donnelle simplification is not considered in this development as it is valid only for short shells. In this way, our theoretical solution is characterized by less limitation to its applications. Exact solutions can be also obtained for unstiffened panels. The related constants are listed as follows:

$D=\frac{E\cdot\delta}{1-\mu^2}$ main slab tension rigidity

$K=\frac{E\cdot\delta^3}{12(1-\mu^2)}$ main slab bending rigidity

For stiffener x and stiffener φ, the constants are

$\bar{\omega}_x=\frac{1}{D_x}\int_{\omega_x}Ed\omega$ $\bar{\omega}_\varphi=\frac{1}{D_\varphi}\int_{\omega_\varphi}Ed\omega$ tension rigidity

$\bar{I}_x=\frac{1}{D_x}\int_{\omega_x}Ez^2d\omega$ $\bar{I}_\varphi=\frac{1}{D_\varphi}\int_{\omega_\varphi}Ez^2d\omega$ lateral bending

$\bar{S}_x=\frac{1}{D_x}\int_{\omega_{f.x}}Ey^2d\omega$ $\bar{S}_\varphi=\frac{1}{D_\varphi}\int_{\omega_{f.\varphi}}Es^2d\omega$ in-plane bending

$\bar{h}_x=\frac{1}{D_x}\int_{\omega_x}Ezd\omega$ $\bar{h}_\varphi=\frac{1}{D_\varphi}\int_{\omega_\varphi}Ezd\omega$ symmetry properties

$\bar{T}_x=\frac{1}{D_x}\frac{E}{12(1+\mu)}(t_{f.x}{}^3\cdot L_{f.x}+t_{w.x}{}^3\cdot L_{w.x})$ uniform torsion

$\bar{T}_\varphi=\frac{1}{D_\varphi}\frac{E}{12(1+\mu)}(t_{f.\varphi}{}^3\cdot L_{f.\varphi}+t_{w.\varphi}{}^3\cdot L_{w.\varphi})$ uniform torsion

Here, E is the modulus of elasticity, μ Poisson's ratio and δ the thickness of the main slab. D_x and D_φ are the intervals of the stiffener x and φ respectively (do not be confused with the following displacement and force state vectors, $\{D_x\}$ and $\{D_\varphi\}$). Note that, the in-plane bending rigidities of the stiffeners are usually interpreted as that for non-uniform torsion or warping. It means that the non-uniform torsion or warping of the stiffeners has been considered in this development.

To describe the boundary conditions and to simplify the following development, we define the displacement and force state vectors related to section x and section φ as:

Displacement State Vector of Section x (θ_x, rotation of section x)

$$(D_x)=(U\quad V\quad W\quad \theta_x)$$

Force State Vector of Section x

$$(F_x)=(N_x\quad N_{x\varphi}\quad R_x\quad M_x)$$

Displacement State Vector of Section φ (θ_φ, rotation of section φ)

$$(D_\varphi)=(U\quad V\quad W\quad \theta_\varphi)$$

Force State Vector of Section φ

$$(F_\varphi)=(N_{\varphi x}\quad N_\varphi\quad R_\varphi\quad M_\varphi)$$

By using these state vectors, boundary conditions of the studied panels can be easily presented. For instance, at boundary $x = x_1$, it may be written as

$$\{D_x\}=[S_x]\cdot\{F_x\}$$

Here, $[S_x]$ is a constant matrix. Free boundary conditions

can be simulated by setting $[S_x]$ equal to zero. Otherwise, if $[S_x]$ is big enough, clamped boundary conditions are automatically simulated.

Direct solutions of Eq.(1) with given boundary conditions are normally very difficult. If SFS is expanded in φ direction, we can write the displacements as (only one term is presented here)

$$\begin{Bmatrix} U(x,\varphi) \\ V(x,\varphi) \\ W(x,\varphi) \end{Bmatrix} = \begin{Bmatrix} U(x)\cdot \mathrm{Sin}(\lambda_m \varphi) \\ V(x)\cdot \mathrm{Cos}(\lambda_m \varphi) \\ W(x)\cdot \mathrm{Sin}(\lambda_m \varphi) \end{Bmatrix} \tag{2}$$

Consequently, the external loads are supposed to be given by

$$\begin{Bmatrix} X(x,\varphi) \\ Y(x,\varphi) \\ Z(x,\varphi) \end{Bmatrix} = \begin{Bmatrix} X(x)\cdot \mathrm{Sin}(\lambda_m \varphi) \\ Y(x)\cdot \mathrm{Cos}(\lambda_m \varphi) \\ Z(x)\cdot \mathrm{Sin}(\lambda_m \varphi) \end{Bmatrix} \tag{3}$$

with $\lambda_m = \dfrac{m\pi}{\varphi_0}$. Substitution of Eq.(2) and Eq.(3) into Eq.(1) leads an ordinary differential equation system.

$$\begin{bmatrix} a_1 & b_1 & c_1 \\ a_2 & b_2 & c_2 \\ a_3 & b_3 & c_3 \end{bmatrix} \cdot \begin{Bmatrix} U(x) \\ V(x) \\ W(x) \end{Bmatrix} = \begin{Bmatrix} -X(x) \\ -Y(x) \\ Z(x) \end{Bmatrix} \tag{4}$$

Here, the operators are changed into those independent of φ. For <u>cylindrical shells</u>, these operators are linear ones with constant coefficients. Therefore, the homogeneous solutions can be assumed as

$$\begin{Bmatrix} U_h(x) \\ V_h(x) \\ W_h(x) \end{Bmatrix} = \begin{Bmatrix} A \\ B \\ C \end{Bmatrix} \cdot e^{\gamma x}$$

Here, A, B and C are non-zero constants. Substituting into the homogeneous equations, i.e.

$$\begin{bmatrix} a_1 & b_1 & c_1 \\ a_2 & b_2 & c_2 \\ a_3 & b_3 & c_3 \end{bmatrix} \cdot \begin{Bmatrix} U_h(x) \\ V_h(x) \\ W_h(x) \end{Bmatrix} = \begin{Bmatrix} 0 \\ 0 \\ 0 \end{Bmatrix}$$

since the differential calculations will be in the form as $a_i U_h(x) = a_i(\gamma)\cdot U_h(x)$ with $a_i(\gamma)$, a polynomial function of γ, we have

$$\begin{bmatrix} a_1(\gamma) & b_1(\gamma) & c_1(\gamma) \\ a_2(\gamma) & b_2(\gamma) & c_2(\gamma) \\ a_3(\gamma) & b_3(\gamma) & c_3(\gamma) \end{bmatrix} \cdot \begin{Bmatrix} A \\ B \\ C \end{Bmatrix} = \begin{Bmatrix} 0 \\ 0 \\ 0 \end{Bmatrix}$$

Because A, B and C are non-zero constants, we obtain an algebraical equation about γ,

$$\begin{vmatrix} a_1(\gamma) & b_1(\gamma) & c_1(\gamma) \\ a_2(\gamma) & b_2(\gamma) & c_2(\gamma) \\ a_3(\gamma) & b_3(\gamma) & c_3(\gamma) \end{vmatrix} = 0$$

Normally, eight complex roots are obtained as α_k +/- i β_k, k = 1, 2, 3 and 4 (here "i" is the imaginary unit), which are defined as eigenvalues. Then, the homogeneous solutions will be

$$S_h(x) = \sum_i (A_i \quad B_i)\cdot[S]\cdot \begin{Bmatrix} \mathrm{Cos}(\beta_i x) \\ \mathrm{Sin}(\beta_i x) \end{Bmatrix} \cdot e^{\alpha_i x} \tag{5}$$

Where, $\begin{Bmatrix} \mathrm{Cos}(\beta_i x) \\ \mathrm{Sin}(\beta_i x) \end{Bmatrix} \cdot e^{\alpha_i x}$ is defined as the eigenfunction vector for each group of eigenvalues, (i = 1, 2, 3, 4). A_i and B_i are the unknown constants of the homogeneous solutions. Total 8 unknown constants are involved. $S_h(x)$ refers to the homogenous solutions of the displacements, $U_h(x)$, $V_h(x)$ and $W_h(x)$. Since other elements can be derived from the displacements. Generally speaking, $S_h(x)$ stands for all the studied elements. And [S] is a constant matrix, which changes from element to element. The introduction of the eigenfunction vector, $\begin{Bmatrix} \mathrm{Cos}(\beta_i x) \\ \mathrm{Sin}(\beta_i x) \end{Bmatrix} \cdot e^{\alpha_i x}$, will greatly facilitates the calculation. For example, we have

$$\frac{d}{dx}\begin{Bmatrix} \mathrm{Cos}(\beta_i x) \\ \mathrm{Sin}(\beta_i x) \end{Bmatrix} \cdot e^{\alpha_i x} = \begin{bmatrix} \alpha_i & -\beta_i \\ \beta_i & \alpha_i \end{bmatrix} \cdot \begin{Bmatrix} \mathrm{Cos}(\beta_i x) \\ \mathrm{Sin}(\beta_i x) \end{Bmatrix} \cdot e^{\alpha_i x}$$

and

$$\int_a^b \begin{Bmatrix} \mathrm{Cos}(\beta_i x) \\ \mathrm{Sin}(\beta_i x) \end{Bmatrix} \cdot e^{\alpha_i x} \cdot dx = \begin{bmatrix} \alpha_i & -\beta_i \\ \beta_i & \alpha_i \end{bmatrix}^{-1} \cdot \begin{Bmatrix} \mathrm{Cos}(\beta_i x) \\ \mathrm{Sin}(\beta_i x) \end{Bmatrix} \cdot e^{\alpha_i x} \Bigg|_a^b$$

For <u>sector plates</u>, by using a transfer function t = ln(x/q) (x = q at the middle of the plate), Eq.(4) changes into

$$\begin{bmatrix} a_1 & b_1 & \frac{1}{x}\cdot c_1 \\ a_2 & b_2 & \frac{1}{x}\cdot c_2 \\ a_3 & b_3 & \frac{1}{x}\cdot c_3 \end{bmatrix} \cdot \begin{Bmatrix} U(t) \\ V(t) \\ W(t) \end{Bmatrix} = \begin{Bmatrix} -x^2\cdot X(t) \\ -x^2\cdot Y(t) \\ x^3\cdot Z(t) \end{Bmatrix}$$

Here, the operators depend only on variable t with constant coefficients. Therefore, the homogeneous solutions will be in the form as

$$\begin{Bmatrix} U_h(t) \\ V_h(t) \\ W_h(t) \end{Bmatrix} = \begin{Bmatrix} \frac{1}{x}\cdot A\cdot e^{\gamma t} \\ \frac{1}{x}\cdot B\cdot e^{\gamma t} \\ C\cdot e^{\gamma t} \end{Bmatrix}$$

For the same reason as the cylindrical shells, we obtain the homogeneous solutions as

$$S_h(t) = \frac{1}{x^k}\sum_i (A_i \quad B_i)\cdot[S]\cdot \begin{Bmatrix} \mathrm{Cos}(\beta_i t) \\ \mathrm{Sin}(\beta_i t) \end{Bmatrix} \cdot e^{\alpha_i t} \tag{6}$$

Note that a k constant is introduced for each element of the sector

plates. For instance, k = 0 for $W_h(t)$, and k = 1 for $U_h(t)$, $V_h(t)$ and so on. Considering that k=0 for all the elements of cylindrical shells, Eq.(5) and Eq.(6) have obviously the same form. For simplification, Eq.(5) and Eq.(6) may be rewritten in the unified form.

$$S_h(x) = \left(\bar{S}_h(x)\right)\cdot\{A\}$$

Here, {A} is defined as the unknown vector (in column, 8x1) of the homogeneous solution. For both sector plates and cylindrical shells, 8 unknowns are involved (for simplification, written in row)

$$(A) = (A_1 \quad B_1 \quad A_2 \quad B_2 \quad A_3 \quad B_3 \quad A_4 \quad B_4)$$

And $\bar{S}_h(x)$ is the basic function vector (1x8) of the homogeneous solution. Taking the first two components of $\bar{S}_h(x)$ as example, for <u>cylindrical shells</u>, they are

$$(1 \quad 0)\cdot[S]\cdot\begin{Bmatrix}\mathrm{Cos}(\beta_1 x)\\ \mathrm{Sin}(\beta_1 x)\end{Bmatrix}\cdot e^{\alpha_1 x} \quad \text{and} \quad (0 \quad 1)\cdot[S]\cdot\begin{Bmatrix}\mathrm{Cos}(\beta_1 x)\\ \mathrm{Sin}(\beta_1 x)\end{Bmatrix}\cdot e^{\alpha_1 x}$$

For <u>sector plates</u>, they are

$$(1 \quad 0)\cdot[S]\cdot\begin{Bmatrix}\mathrm{Cos}(\beta_1 t)\\ \mathrm{Sin}(\beta_1 t)\end{Bmatrix}\cdot\frac{e^{\alpha_1 t}}{x^k} \quad \text{and} \quad (0 \quad 1)\cdot[S]\cdot\begin{Bmatrix}\mathrm{Cos}(\beta_1 t)\\ \mathrm{Sin}(\beta_1 t)\end{Bmatrix}\cdot\frac{e^{\alpha_1 t}}{x^k}$$

If the external loads in Eq.(4) are given by

$$\begin{Bmatrix}X(x)\\ Y(x)\\ Z(x)\end{Bmatrix} = \begin{bmatrix}P_{x1} & P_{x2} & P_{x3} & P_{x4}\\ P_{y1} & P_{y2} & P_{y3} & P_{y4}\\ P_{z1} & P_{z2} & P_{z3} & P_{z4}\end{bmatrix}\cdot\begin{Bmatrix}1\\ x\\ x^2\\ x^3\end{Bmatrix}$$

we may write the particular solutions for both the sector plates and cylindrical shells as

$$S_p(x) = \left(\bar{S}_p(x)\right)\cdot\{P\}$$

Here, $\bar{S}_p(x)$ is the unit load solution vector (1x12) of the element S(x), and {P} is a constant vector (12x1) of the external load coefficients (written in row) as follows.

$$(P) = \left((P_x) \quad (P_y) \quad (P_z)\right)$$

$$\text{and}\begin{cases}(P_x) = (P_{x1} \quad P_{x2} \quad P_{x3} \quad P_{x4})\\ (P_y) = (P_{y1} \quad P_{y2} \quad P_{y3} \quad P_{y4})\\ (P_z) = (P_{z1} \quad P_{z2} \quad P_{z3} \quad P_{z4})\end{cases}$$

At last, the general solutions for both panels are obtained by the combination of the homogeneous solution and the particular solution of external loads, i.e.

$$S(x) = \left(\bar{S}_h(x)\right)\cdot\{A\} + \left(\bar{S}_p(x)\right)\cdot\{P\} \qquad (7)$$

Totally, 8 unknown homogeneous constants, {A}, are involved in Eq.(7), which are determined by the connection of the panels of the structure or the boundary conditions in section x. Based on the SFS expansion in the circumferential direction, boundary φ is simply supported.

2.2 FUNDAMENTAL SOLUTIONS OF THE STRUCTURE

By using the general solution of Eq.(7), at the departure end, $x = x_1$, and at the arrival end, $x = x_2$, we have the displacement state vector {D} and the force state vector {F} as

$$\begin{aligned}\{D\}_1 &= [G]_1\cdot\{A\} + [H]_1\cdot\{P\}\\ \{D\}_2 &= [G]_2\cdot\{A\} + [H]_2\cdot\{P\}\\ \{F\}_1 &= [Q]_1\cdot\{A\} + [R]_1\cdot\{P\}\\ \{F\}_2 &= [Q]_2\cdot\{A\} + [R]_2\cdot\{P\}\end{aligned} \qquad (8)$$

Here, $[G]_1$ $[G]_2$ $[Q]_1$ $[Q]_2$ are constant matrices (4x8), and $[H]_1$ $[H]_2$ $[R]_1$ $[R]_2$ are constant matrices (4x12). In fact, 4 systems are involved in Eq.(8), and each has 4 equations.

The first two equation systems in Eq.(8) lead a solution for the homogeneous unknowns

$$\{A\} = [G]\cdot\{D\} + [H]\cdot\{P\}$$

$$\text{with} \qquad \{D\} = \begin{Bmatrix}\{D\}_1\\ \{D\}_2\end{Bmatrix}$$

By this way, the general solutions of the studied panel, Eq.(7), will depend on 8 node displacements {D} instead of {A}. Note that, for a given panel, [G] and [H] are constant matrices of 8x8 and 8x12 respectively (do not be confused with $[G]_1$ $[G]_2$ and $[H]_1$ $[H]_2$). Substituting {A} into the last two equation systems in Eq.(8) results in

$$\{F\} = [Q]\cdot\{D\} + [R]\cdot\{P\}$$

$$\text{with} \qquad \{F\} = \begin{Bmatrix}\{F\}_1\\ \{F\}_2\end{Bmatrix} \qquad (9)$$

Again, [Q] and [R] are 8x8 and 8x12 matrices, and different from $[Q]_1$ $[Q]_2$ and $[R]_1$ $[R]_2$ in Eq.(8).

Equation.(9) gives out the internal forces at the two end sections of each panel. By the equilibrium equations at each node of the structure where the panels are connected, the final system of the structure is formed as

$$[A]\cdot\{D\} = [B]\cdot\{P\} \qquad (10)$$

It should be aware that, in Eq.(10), {D} stands for node displacements of the whole structure, and {P} stands for all the coefficients of the external loads on each panel. [A] and [B] are the rigidity matrix and the load matrix of the structure. If the structure is composed of M panels with N nodes, [A] is in 4Nx4N, and [B] in 4Nx12M. Eq.(10) stands for a system with 4N equations. The similar system obtained by FEM analysis will be much greater than it.

In general, at some nodes, reaction forces from support may be also included, which can be written as

$$\{F\}_n = [S]_n\cdot\{D\}_n \qquad (11)$$

Here $[S]_n$ stands for the rigidity matrix of the node. In the node equilibrium equations(by which Eq.(10) is formed from Eq.(9)), $\{F\}_n$ should be also included together with the panel force {F} in Eq.(9). By this means, the support conditions at each node can vary

arbitrarily.

It is clear that after solving the system of Eq.(10), the general solutions of each panel are determined. For detailed studies of the structure, the general solutions on each unit load coefficient (i.e. setting P_{x1}, P_{x2}, P_{x3}, P_{x4}, P_{y1}, P_{y2}, P_{y3}, P_{y4}, P_{z1}, P_{z2}, P_{z3}, P_{z4} = 1 separately) are defined as the fundamental solution of the structure for each SFS term. It can be seen that the fundamental solution may be written as a vector (1x12M), $\vec{S}_F(x)$, by which the general solution is in the form as

$$S_m(x) = \left(\vec{S}_F(x)\right)_m \cdot \{P\}_m \qquad (12)$$

Here, $\{P\}_m$ has the same meaning as $\{P\}$ in Eq.(10). The subscribe "m" indicates the m^{th} term of SFS expansion.

2.3 SUPERPOSITION OF THE FUNDAMENTAL SOLUTIONS

The usual loads in hydraulic and maritime engineering are water pressures. For the studied panels, it is the lateral load Z. For horizontally curved structures, it is independent of coordinate φ and uniform or linear in coordinate x, i.e.

$$Z(x,\varphi) = a + b\cdot x = \sum_{m=1}^{\infty} \frac{4\cdot(a+b\cdot x)}{(2m-1)\cdot\pi} \cdot \mathrm{Sin}\left[\frac{(2m-1)\cdot\pi}{\varphi_0}\cdot\varphi\right]$$

Comparing with Eq.(2) and Eq.(3), we may use

$$\lambda_m = \frac{(2m-1)\cdot\pi}{\varphi_0} \qquad (13)$$

It means that only odd terms of the SFS expansion are valid. The external load coefficients are

$$P_{z1} = \frac{4\cdot a}{(2m-1)\cdot\pi} \qquad P_{z1} = \frac{4\cdot b}{(2m-1)\cdot\pi} \qquad (14)$$

Other coefficients of the external loads are zero. Then, the final solution will be given by

$$S(x,\varphi) = \sum_{m=1}^{\infty}\left[S_{P_{z1}}(x)\cdot P_{z1} + S_{P_{z1}}(x)\cdot P_{z2}\right]\cdot\begin{Bmatrix}\mathrm{Cos}(\lambda_m\varphi)\\ \mathrm{Sin}(\lambda_m\varphi)\end{Bmatrix} \qquad (15)$$

Here, $S_{P_{z1}}(x)$ and $S_{P_{z2}}(x)$ stand for the fundamental solutions of the external loads P_{z1} and P_{z2} of the m^{th} SFS term. Sine and cosine functions are selected with respect to the element. Generally, the number of SFS terms are depended on the accuracy expected as well as the forms of the external loads. For uniform water pressure in coordinate φ, a maximum of 13 terms is enough to provide a high level of accuracy.

3. DOUBLE-SKINNED CYLINDRICAL GATE

3.1 DIMENSIONS

The gate is designed to support a maximum water pressure of 80m (water level difference between the upstream canal and the downstream canal, see Fig.1). The chamber of the ship lock is 15m wide, and the downstream tunnel is 12.5m high (with 5m water and 7.5m clearance). The length of the cylindrical gate in circumferential direction is defined as L, and the thickness, D, is the distance between upstream skin and downstream skin, see Fig.4.

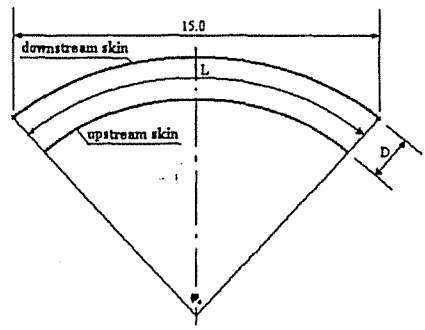

Fig.4 Length and Thickness of the Gate

Therefore, we have

$$L = \left[\frac{7.5}{\mathrm{Sin}(\varphi_0/2)} - \frac{D}{2}\right]\cdot\varphi_0$$

The calculation of L with φ_0 from 0° to 180° and D = 2, 3, 4 m respectively is shown in Fig.5.

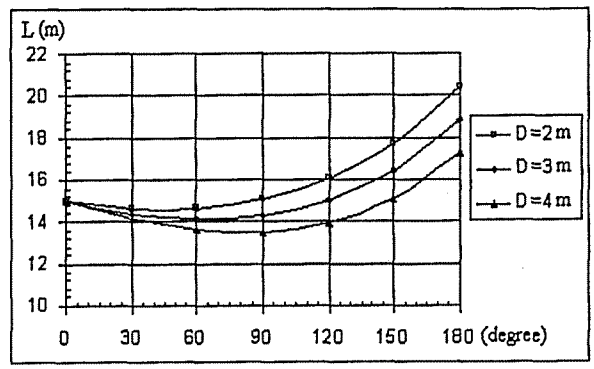

Fig.5 Variation of the Length with the Thickness and Central Angle

It shows that the curved structure does not always increase the length (except the changes of the boundary diaphragms and the support arrangement). In this paper, we use D = 3 m, and the central angle φ_0 varies from 0° to 120°. Water pressure is acting on the downstream skin. Downstream seal system (lateral seals, top and bottom seals) is adopted.

3.2 MODEL OF THE STIFFENED PANEL METHOD

An assembly of 16 panels is employed to model this double skinned gate, see Fig.2. The 16 panels are connected with 12 joints (nodes). Therefore, the number of DOFs in Eq.(10) is only 48. Each panel is reinforced with stiffeners in both generator and circumferential directions. Typical panels are shown in Fig.3 (panel 3: stiffened cylindrical shell under water pressure; panel 4: stiffened sector plate, middle diaphragm). Detailed scantling of the gate is not included in this paper. The vertical diaphragms at $\varphi = 0$ and $\varphi = \varphi_0$ are simulated with the simply supported boundary conditions for each studied panel. Using SFS expansion in the

circumferential direction, this simply supported boundary conditions are automatically satisfied. At the top and bottom seals, the gate is supposed to be constrained against normal downward displacements. This is simulated by the node rigidity in Eq.(11). As a comparison, free seal conditions are also simulated by setting the node rigidity in Eq.(11) being zero. Those two conditions are referred as **seal free** and **seal constrained** conditions in the following presentation.

3.3 DISPLACEMENTS AND STRESSES

Displacements and stresses are presented on the transverse section for the two conditions: **seal free** and **seal constrained.** Two extreme central angles, $\varphi_0 = 0°$ and $\varphi_0 = 120°$, are presented for comparison from Fig.6 to Fig.9). With respect to each panel, the transverse stress is defined as the normal stress in the generator direction, and the circumferential stress is in the circumferential direction. The transverse displacements are the displacements parallel to the transverse section, while the circumferential displacements are those normal to the transverse section. For all the computation cases of $\varphi_0 = 0°$, 30°, 60°, 90° and 120° (with the same scantling), the maximum values of the studied terms are listed in Tab.1, in which W_{max} , V_{max} , $\sigma_{x\text{-}max}$ and $\sigma_{y\text{-}max}$ are defined as the maximum values of the transverse and circumferential displacements, and the transverse and circumferential stresses respectively.

Tab.1 Maximum Values of the Studied Terms

Seal Constrained					
φ_0	L	W_{max}	V_{max}	$\sigma_{x\text{-}max}$	$\sigma_{y\text{-}max}$
degree	m	m	m	N/m^2	N/m^2
0	15.000	0.0146	0.0022	211	116
30	14.387	0.0140	0.0043	213	114
60	14.137	0.0140	0.0064	231	117
90	14.305	0.0142	0.0085	264	149
120	14.996	0.0138	0.0102	291	195
Seal Free					
φ_0	L	W_{max}	V_{max}	$\sigma_{x\text{-}max}$	$\sigma_{y\text{-}max}$
degree	m	m	m	N/m^2	N/m^2
0	15.000	0.0238	0.0046	103	189
30	14.387	0.0230	0.0082	90	209
60	14.137	0.0279	0.0143	99	269
90	14.305	0.0467*	0.0306	162	416*
120	14.996	0.1367*	0.1065*	378*	907*

* Values are not acceptable.

From Tab.1 and the figures (Fig.6 to Fig.9), it can be seen that, in the **seal free** condition, the gate behaves like a curved box beam. The circumferential stress is always greater than the transverse stress. The stresses in the downstream skin are in tension, and the stresses in the upstream skin are in compression. While the circumferential stress and displacement, $\sigma_{y\text{-}max}$ and V_{max} , increase greatly with the central angle φ_0 , the transverse stress and displacement, $\sigma_{x\text{-}max}$ and W_{max} will first decrease with the central angle φ_0 because of the decrease of the length. Then, they increase quickly because of the curvature and the increase of the length. In the curved situation, the circumferential stresses in the middle diaphragms are not linearly distributed (seal free, $\varphi_0 = 120°$ in Fig.9), which means that for curved box beams, if the traditional beam theory is used, the non-linearly distributed normal stress on the web have to be considered. The famous effective width method can only correct the shear lag effects on the flange (upstream and downstream skins in this paper). In the case of $\varphi_0 = 120°$, both the stresses and displacements in the seal free condition are not acceptable (the same scantling being the same for all the cases).

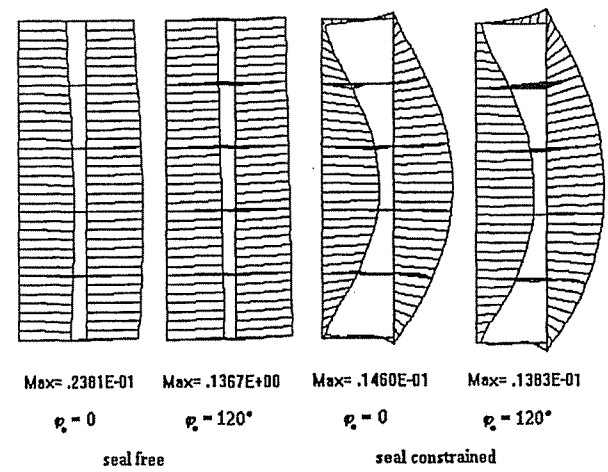

Fig.6 Transverse Displacements of the Middle Section ($\varphi = \varphi_0/2$)

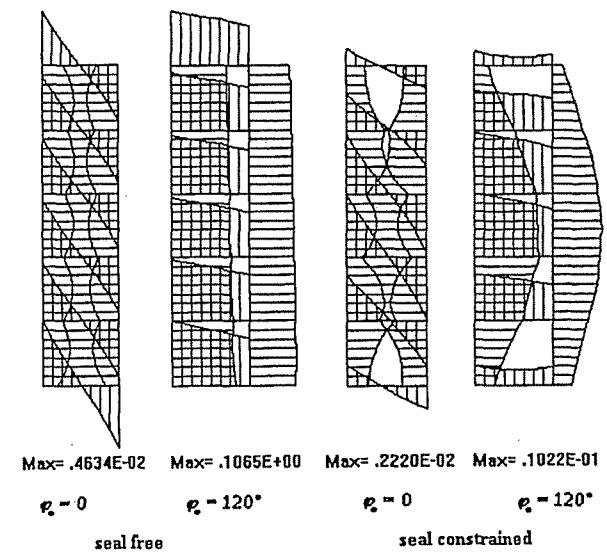

Fig.7 Circumferential Displacements of the Boundary Section ($\varphi = 0$)

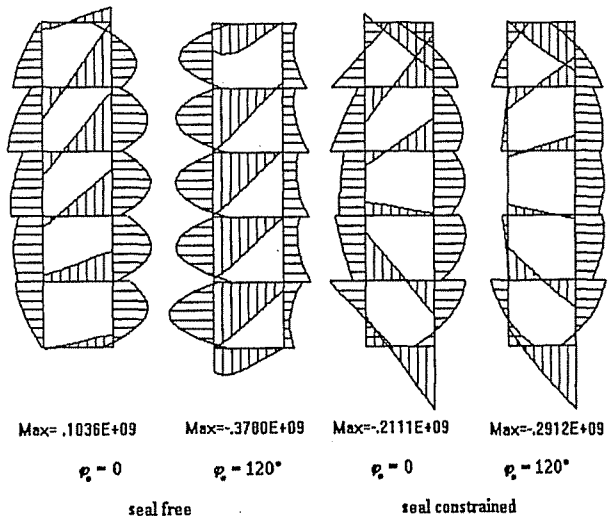

Fig.8 Transverse Stresses of the Main Slab on the Middle Section ($\varphi = \varphi_0/2$)

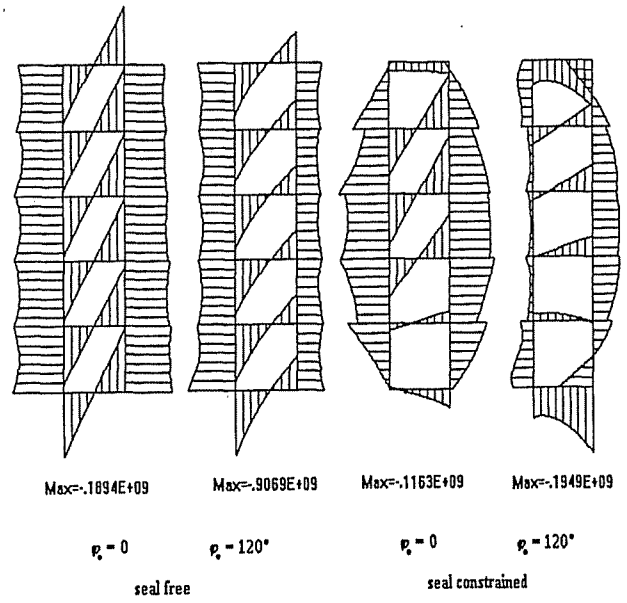

Fig.9 Circumferential Stresses of the Main Slab on the Middle Section ($\varphi = \varphi_0/2$)

When the seal constrained condition is considered, the maximum transverse displacement, W_{max}, will not change too much from $\varphi_0 = 0°$ to $\varphi_0 = 120°$ (from 0.0146m to 0.0138m). The circumferential displacement, V_{max} , increases from 0.0022m to 0.0102m, but the value is still acceptable. The stresses have the same trends as V_{max} . When the central angle changes from 0° to 120°, $\sigma_{x\text{-}max}$ increases from 211 to 291 N/m^2, while $\sigma_{y\text{-}max}$ increases from 116 to 195 N/m^2.

It should be noted that, if the downstream tunnel of the ship locks is too high (depends on navigation requirements), the downstream gate may be designed into several independent sections. In the practical working conditions, one is put above another. In that case, seal free conditions may be much closer to the real situations. Then for curved structures, more materials for the gate will be needed to reduce the displacements and stresses. Another economical solution may be to constrain the circumferential displacement (V) at the two boundaries, $\varphi = 0$ and φ_0, by using special gate slots (see Fig.1). This alternative will be studied in the future.

4. CONCLUSIONS

- The Stiffened Panel Method for curved structures is developed and applied to design a double skinned cylindrical gate for high rise ship locks with a water head of 80m. Only 48 DOFs (degrees of freedom) are needed, which clearly demonstrate the advantages of this method.
- For large central angles, top and bottom seal constrained conditions have to be considered in order to make both the displacements and stresses are acceptable without increasing the scantling. Otherwise, the circumferential displacements may be constrained by specially designed gate slots at the boundary. It will break the limitation to the simply supported conditions automatically simulated by the SFS expansion in the circumferential direction.

REFERENCES

Dehousse N. M., 1989, "Very High Rise Navigation Locks", Bulletin of the Permanent International Association of Navigation Congress, N°.67.

Dehousse, N. M. 1961, "Les Bordages Radis en Construction Hydraulique", Mémoires du Centre d'Etudes, de Recherche et d'Essais Scientifiques de Génie Civil (Nouvelle Série), Vol.1, Univ. de Liége, Belgique.

Dehousse N. M. and Deprez J. 1967, "Les Bordage Orthotropes Plans", Calcul d'une Porte d'écluse, Mémoires du CERES (Nouvelle série) n°22.

Hatzidakis, N. and Michael M. Bernitsas 1994, "Comparative Design of Orthogonally Stiffened Plates for Production and Structural Integrity" - Part 1: Size Optimization; - part 2: Shape Optimization, Journal of Ship Production, Volume 10, No.3.

Hengfeng, wang 1997, "Effective Unitary Force Method for Stiffened Panels", Report of ANAST, University of Liege, Belgium.

Rigo Ph. 1992, "Stiffened Sheathings of Orthotropic Cylindrical Shells", Journal of Structure Engineering, ASCE, Vol.118, No.4, April 1992.

Rigo Ph. 1989, "Applications des Développements Harmoniques au Calcul des Ouvrages Hydrauliques Métalliques", Collection des publications de la Faculté des Sciences Appliquées de l'Université de Liège, No.120.